Engineering Science and Technology, an International Journal xxx (2016) xxx–xxx

HOSTED BY

ELSEVIER

Contents lists available at ScienceDirect

Engineering Science and Technology, an International Journal

journal homepage: www.elsevier.com/locate/jestch

Full Length Article

A novel hybrid Particle Swarm Optimizer with multi verse optimizer for global numerical optimization and Optimal Reactive Power Dispatch problem

Pradeep Jangir [a], Siddharth A. Parmar [a], Indrajit N. Trivedi [b], R.H. Bhesdadiya [a]

[a] Department of Electrical Engineering, Lukhdhirji Engineering College, Morbi, Gujarat 363641, India
[b] Department of Electrical Engineering, Government Engineering College, Gandhinagar, Gujarat 389001, India

ARTICLE INFO

Article history:
Received 26 September 2016
Accepted 16 October 2016
Available online xxxx

Keywords:
Benchmark function
Optimal Reactive Power Dispatch
Voltage stability
Power system
Hybrid PSO-MVO
Constraints

ABSTRACT

Recent trend of research is to hybridize two and more algorithms to obtain superior solution in the field of optimization problems. In this context, a new technique hybrid Particle Swarm Optimization (PSO)-Multi verse Optimizer (MVO) is exercised on some unconstraint benchmark test functions and the most common problem of the modern power system named Optimal Reactive Power Dispatch (ORPD) is optimized using the novel hybrid meta-heuristic optimization algorithm Particle Swarm Optimization-Multi Verse Optimizer (HPSO-MVO) method. Hybrid PSO-MVO is combination of PSO used for exploitation phase and MVO for exploration phase in uncertain environment. Position and Speed of particle is modernised according to location of universes in each iteration. The hybrid PSO-MVO method has a fast convergence rate due to use of roulette wheel selection method. For the ORPD solution, standard IEEE-30 bus test system is used. The hybrid PSO-MVO method is implemented to solve the proposed problem. The problems considered in the ORPD are fuel cost reduction, Voltage profile improvement, Voltage stability enhancement, Active power loss minimization and Reactive power loss minimization. The results obtained with hybrid PSO-MVO method is compared with other techniques such as Particle Swarm Optimization (PSO) and Multi Verse Optimizer (MVO). Analysis of competitive results obtained from HPSO-MVO validates its effectiveness compare to standard PSO and MVO algorithm.

1. Introduction

At the present time, hybridize of two and more algorithms to obtain superior solution in the field of optimization problems and application in The Optimal Reactive Power Dispatch (ORPD) is very significant problem and most focused objective for power system planning and operation [1]. The ORPD is the elementary tool which permits the utilities to identify the economic operational and much secure states in the system [2,3]. The ORPD problem is one of the utmost operating desires of the electrical power system [4]. The prior function of ORPD problem is to evaluate the optimum operational state for Bus system by minimizing each objective function within the limits of the operational constraints like equality constraints and inequality constraints [5]. Hence the Optimal Reactive Power Dispatch problem can be defined as an extremely non-linear and non-convex multimodal optimisation problem [6].

From the past few years too many optimization techniques were used for the solution of the Optimal Reactive Power Dispatch (ORPD) problem. Some traditional methods are used to solve the proposed problem have been suffered from some limitations like converging at local optima, not suitable for binary or integer problems and also have the assumptions like the convexity, differentiability, and continuity [7]. Hence these techniques are not suitable for the actual ORPD situation [8,9]. All these limitations are overcome by meta-heuristic optimization methods like genetic algorithm (GA), Particle Swarm Optimization algorithm (PSO), ant colony algorithm (ACO), differential evolution algorithm (DEA) and harmony search algorithm (HSA) [10,11].

In the present work, a newly introduced hybrid meta-heuristic optimisation technique named Hybrid Particle Swarm Optimization-Multi Verse Optimizer (HPSO-MVO) is applied to solve the Optimal Reactive Power Dispatch problem. HPSO-MVO comprises of best characteristic of both Particle Swarm Optimization [12] and Multi Verse Optimizer [13] algorithm. The

E-mail addresses: pkjmtech@gmail.com (P. Jangir), saparmar92@gmail.com (S.A. Parmar), forumtrivedi@gmail.com (I.N. Trivedi), rhblec@gmail.com (R.H. Bhesdadiya).

Peer review under responsibility of Karabuk University.

http://dx.doi.org/10.1016/j.jestch.2016.10.007
2215-0986/

capabilities of HPSO-MVO are finding the near global solution, fast convergence rate due to use of roulette wheel selection, can handle continuous and discrete optimization problems.

In this work, the HPSO-MVO is implemented to unconstraint bench mark function and standard IEEE-30 bus test system [14] to solve the ORPD [15–20] problem. There are five objective cases considered in this paper that has to be optimize using HPSO-MVO technique are Fuel Cost Reduction, Voltage Stability Improvement, Voltage Deviation Minimization, Active Power Loss Minimization and Reactive Power Loss Minimization. The result shows the optimal adjustments of control variables in accordance with their limits. The results obtained using HPSO-MVO technique has been compared with standard Particle Swarm Optimisation (PSO) and Multi Verse Optimizer (MVO) techniques. The results show that HPSO-MVO gives better optimization values as compared to other methods which proves the effectiveness of the proposed algorithm.

The structure of the paper can be given as follow: – Section 1 consists of Introduction, Section 2 includes description of participated algorithms, Section 3 consists of competitive results analysis of unconstraint test benchmark problem and ORPD problem finally acknowledgement and conclusion based on results is drawn.

2. Standard PSO and standard MVO

2.1. Particle Swarm Optimization

The Particle Swarm Optimization algorithm (PSO) was discovered by James Kennedy and Russell C. Eberhart in 1995 [12]. This algorithm is inspired by simulation of social psychological expression of birds and fishes. PSO includes two terms P_{best} and G_{best}. Position and velocity are updated over the course of iteration from these mathematical equations:

$$v_{ij}^{t+1} = w v_{ij}^{t} + c_1 R_1 (Pbest^t - X^t) + c_2 R_2 (Gbest^t - X^t) \tag{1}$$

$$X^{t+1} = X^t + v^{t+1} (\mathrm{i} = 1, 2 \ldots \mathrm{NP}) \text{ And } (\mathrm{j} = 1, 2 \ldots \mathrm{NG}) \tag{2}$$

where

$$w = w^{\max} - \frac{(w^{\max} - w^{\min}) * iteration}{\max iteration}, \tag{3}$$

w^{max} = 0.4 and w^{min} = 0.9. v_{ij}^{t}, v_{ij}^{t+1} Is the velocity of jth member of ith particle at iteration number (t) and (t + 1). (Usually $C_1 = C_2 = 2$), r_1 and r_2 Random number (0, 1).

2.2. Multi-verse optimizer

Three notions such as black hole, white hole and wormhole shown in Fig. 1 are the main motivation of the MVO algorithm. These three notions are formulated in mathematical models to evaluate exploitation, exploration and local search, respectively. The white hole assumed to be the main part to produce universe. Black holes are attracting all due to its tremendous force of gravitation. The wormholes behave as time/space travel channels in which objects can moves rapidly in universe. Main steps uses to the universes of MVO [13]:

I. If the inflation rate is greater, the possibility of presence of white hole is greater.
II. If the inflation rate is greater, the possibility of presence of black hole is lower.
III. Universes having greater inflation rate are send the substances through white holes.
IV. Universes having lesser inflation rate are accepting more substances through black holes.

The substances/objects in every universe can create random movement in the direction of the fittest universe through worm holes irrespective to the inflation rate. The objects are move from a universe having higher inflation rate to a universe having lesser inflation rate. It can assure the enhancement of the average inflation rates of the entire cosmoses with the iterations. In each iteration, the universes are sorted according to their inflation rates and select one from them using the roulette wheel as a white hole. The subsequent stages are used for this procedure. Assume that

$$U = \begin{bmatrix} x_1^1 & x_1^2 & \cdot & \cdot & x_1^d \\ x_2^1 & x_2^2 & \cdot & \cdot & x_2^d \\ \cdot & \cdot & \cdot & \cdot & \cdot \\ \cdot & \cdot & \cdot & \cdot & \cdot \\ x_n^1 & x_n^2 & \cdot & \cdot & x_n^d \end{bmatrix} \tag{4}$$

Where, d shows the No. of variables and n shows the No. of candidate solutions:

$$x_i^j = \begin{cases} x_k^j; & r1 < NI(Ui) \\ x_i^j; & r1 \geqslant NI(Ui) \end{cases} \tag{5}$$

where, x_i^j shows the jth variable of ith universe, U_i indicates the ith universe, $NI(U_i)$ is normalized inflation rate of the ith universe, $r1$ is a random No. from [0,1], and x_k^j shows the jth variable of kth universe chosen through a roulette wheel. To deliver variations for all universe and more possibility of increasing the inflation rate by worm holes, suppose that worm hole channels are recognized among a universe and the fittest universe created until now. This mechanism is formulated as:

$$x_i^j = \begin{cases} \begin{cases} X_j + TDR \times ((ub_j - lb_j) \times r4 + lb_j); r3 < 0.5 \\ X_j - TDR \times ((ub_j - lb_j) \times r4 + lb_j); r3 \geqslant 0.5 \end{cases}; r2 < WEP \\ x_i^j; r2 \geqslant WEP \end{cases} \tag{6}$$

where X_j shows jth variable of fittest universe created until now, lb_j indicates the min limit of jth parameter, ub_j indicates max limit of jth parameter, x_i^j shows the jth parameter of ith universe, and r2, r3, r4 are random numbers from [0, 1]. It can be concluded by the formulation that wormhole existence probability (WEP) and travelling distance rate (TDR) are the chief coefficients. The formula for these coefficients are given by:

$$WEP = \min + l \times \left(\frac{\max - \min}{L} \right) \tag{7}$$

Where, l shows the present run, and L represent maximum run number/iteration.

$$TDR = 1 - \frac{l^{1/p}}{L^{1/p}} \tag{8}$$

Where, p states the accuracy of exploitation with the iterations. If the p is greater, the exploitation is faster and more precise. The complexity of the MVO algorithms based on the No. of iterations, No. of universes, roulette wheel mechanism, and universe arranging mechanism. The overall computational complexity is as follows:

$$O(MVO) = O(l(O(Quicksort) + n \times d \times (O(roulette\_wheel)))) \tag{9}$$

$$O(MVO) = O(l(n^2 + n \times d \times \log n)) \tag{10}$$

Where, n shows No. of universes, l shows the maximum No. of run/iterations, and d shows the No. of substances.

Please cite this article in press as: P. Jangir et al., A novel hybrid Particle Swarm Optimizer with multi verse optimizer for global numerical optimization and Optimal Reactive Power Dispatch problem, Eng. Sci. Tech., Int. J. (2016), http://dx.doi.org/10.1016/j.jestch.2016.10.007

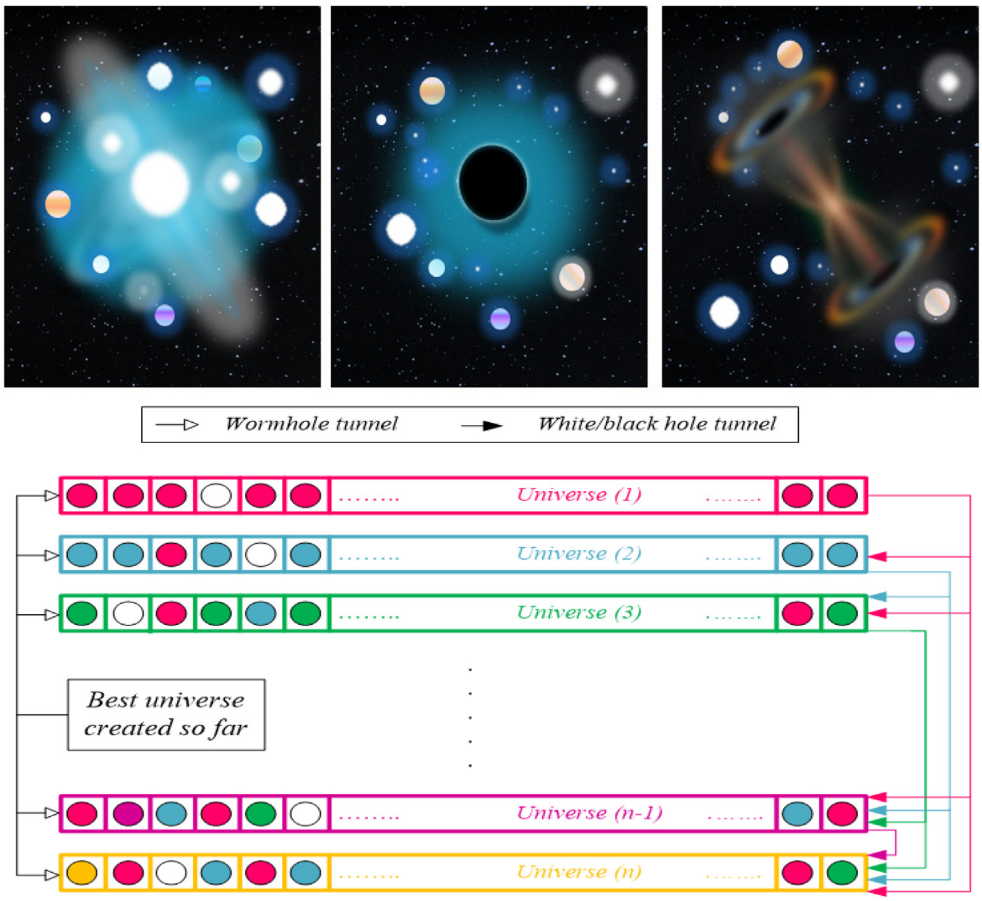

Fig. 1. Basic principle of MVO.

3. The hybrid PSO-MVO algorithm

A set of Hybrid PSO-MVO is combination of separate PSO and MVO. Hybrid PSO-MVO merges the best strength of both PSO in exploitation and MVO in exploration phase towards the targeted optimum solution when replace Pbest Value of PSO with Universe value of MVO.

$$v_{ij}^{t+1} = w v_{ij}^{t} + c_1 R_1 (Universes^{t} - X^{t}) + c_2 R_2 (Gbest^{t} - X^{t}) \quad (11)$$

4. Optimal Reactive Power Dispatch problem formulation

As specified before, ORPD is Optimized problem of power flow that provides the optimum values of independent variables by optimizing a predefined objective function with respect to the operating bounds of the system [1]. The ORPD problem can be mathematically expressed as a non-linear constrained optimization problem as follows [1]:

$$\text{Minimize } f(a,b) \quad (12)$$

$$\text{Subject to } s(a,b) = 0 \quad (13)$$

$$\text{And } h(a,b) \leqslant 0 \quad (14)$$

where, a = vector of state variables, b = vector of control variables, $f(a,b)$ = objective function, $s(a,b)$ = *different* equality constraints set, $h(a,b)$ = different inequality constraints set.

4.1. Variables

4.1.1. Control variables

The control variables should be adjusted to fulfill the power flow equations. For the ORPD problem, the set for control variables can be formulated as [1,5]:

$$b^T = [P_{G_2} \cdots P_{G_{NGen}},\ V_{G_1} \cdots V_{G_{NGen}}, Q_{C_1} \cdots Q_{C_{NCom}},\ T_1 \cdots T_{NTr}] \quad (15)$$

where,

P_G = Real power output at the *PV* (*Generator*) buses excluding at the slack (Reference) bus.
V_G = Magnitude of Voltage at *PV* (*Generator*) buses.
Q_C = shunt *VAR* compensation.
T = tap settings of transformer.

NGen, NTr, NCom = No. of generator units, No. of tap changing transformers and No. of shunt *VAR* compensation devices, respectively.

4.1.2. State variables

There is a need of variables for all ORPD formulations for the characterization of the Electrical Power Engineering state of the system. So, the state variables can be formulated as [1,5]:

$$a^T = [P_{G_1}, V_{L_1} \cdots V_{L_{NLB}},\ Q_{G_1} \cdots Q_{G_{NGen}},\ S_{l_1} \cdots S_{l_{Nline}}] \quad (16)$$

where,

P_{G_1} = Real power generation at reference bus.
V_L = Magnitude of Voltage at Load buses.

Please cite this article in press as: P. Jangir et al., A novel hybrid Particle Swarm Optimizer with multi verse optimizer for global numerical optimization and Optimal Reactive Power Dispatch problem, Eng. Sci. Tech., Int. J. (2016), http://dx.doi.org/10.1016/j.jestch.2016.10.007

Q_G = Reactive power generation of all generators.
S_l = Transmission line loading.

NLB, Nline = No. of *PQ* buses and the No. of transmission lines, respectively.

4.2. Constraints

There are two ORPD constraints named inequality and equality constraints. These constraints are explained in the sections given below.

4.2.1. Equality constraints

The physical condition of the power system is described by the equality constraints of the system. These equality constraints are basically the power flow equations which can be explained as follows [1,5].

4.2.1.1. Real power constraints. The real power constraints can be formulated as follows:

$$P_{Gi} - P_{Di} - V_i \sum_{J=i}^{NB} V_j [G_{ij} Cos(\delta_{ij}) + B_{ij} Sin(\delta_{ij})] = 0 \quad (17)$$

4.2.1.2. Reactive power constraints. The reactive power constraints can be formulated as follows:

$$Q_{Gi} - Q_{Di} - V_i \sum_{J=i}^{NB} V_j [G_{ij} Cos(\delta_{ij}) + B_{ij} Sin(\delta_{ij})] = 0 \quad (18)$$

where, $\delta_{ij} = \delta_i - \delta_j$

Where, *NB* = total No. of buses, P_G = real power output, Q_G = reactive power output, P_D = active power load demand, Q_D = reactive power load demand, B_{ij} and G_{ij} = elements of the admittance matrix $Y_{ij} = (G_{ij} + jB_{ij})$ shows the susceptance and conductance between bus i and *j*, respectively.

4.2.2. Inequality constraints

The boundaries of power system devices together with the bounds created to surety system security are given by inequality constraints of the ORPD [5,6].

4.2.2.1. Generator constraints. For all generating units including the reference bus: voltage, real power and reactive power outputs should be constrained within its minimum and maximum bounds as given below:

$$V_{G_i}^{lower} \leqslant V_{G_i} \leqslant V_{G_i}^{upper}, \quad i = 1, \ldots, NGen \quad (19)$$

$$P_{G_i}^{lower} \leqslant P_{G_i} \leqslant P_{G_i}^{upper}, \quad i = 1, \ldots, NGen \quad (20)$$

$$Q_{G_i}^{lower} \leqslant Q_{G_i} \leqslant Q_{G_i}^{upper}, \quad i = 1, \ldots, NGen \quad (21)$$

4.2.2.2. Transformer constraints. Tap settings of transformer should be constrained inside their stated minimum and maximum bounds as follows:

$$T_{G_i}^{lower} \leqslant T_{G_i} \leqslant T_{G_i}^{upper}, \quad i = 1, \ldots, NGen \quad (22)$$

4.2.2.3. Shunt VAR compensator constraints. Shunt VAR compensation devices need to be constrained within its minimum and maximum bounds as given below:

$$Q_{C_i}^{lower} \leqslant Q_{GC_i} \leqslant Q_{C_i}^{upper}, \quad i = 1, \ldots, NGen \quad (23)$$

4.2.2.4. Security constraints. These comprises the limits of magnitude of voltage at *PQ* buses and loadings on transmission line. Voltage for every *PQ* bus should be limited by their minimum and maximum operational bounds. Line flow over each lines should not exceeds its maximum loading limit. So, these limitations can be mathematically expressed as follows [7]:

$$V_{L_i}^{lower} \leqslant V_{L_i} \leqslant V_{L_i}^{upper}, \quad i = 1, \ldots, NGen \quad (24)$$

$$S_{l_i} \leqslant S_{l_i}^{upper}, i = 1, \ldots, Nline \quad (25)$$

The control variables are self-constraint. The inequality constrained of state variables comprises magnitude of *PQ* bus voltage, active power production at reference bus, reactive power production and loadings on line may be encompassed into an objective function in terms of quadratic penalty terms. In which, the penalty

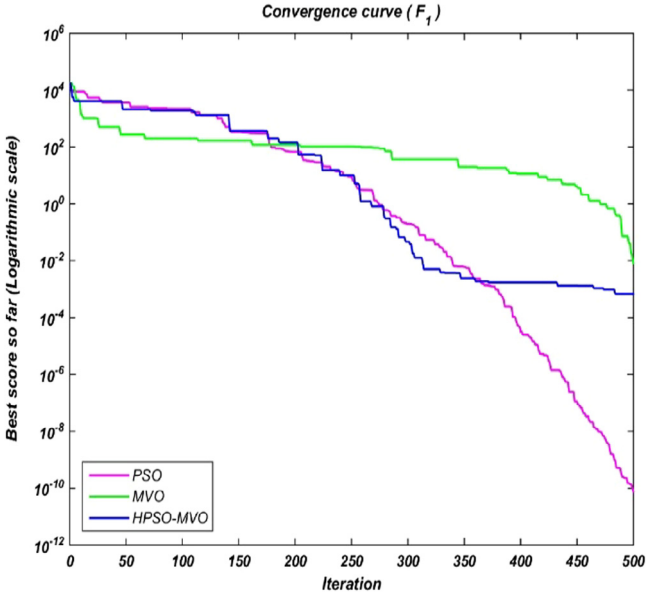

Fig. 2. Convergence curve of function F1.

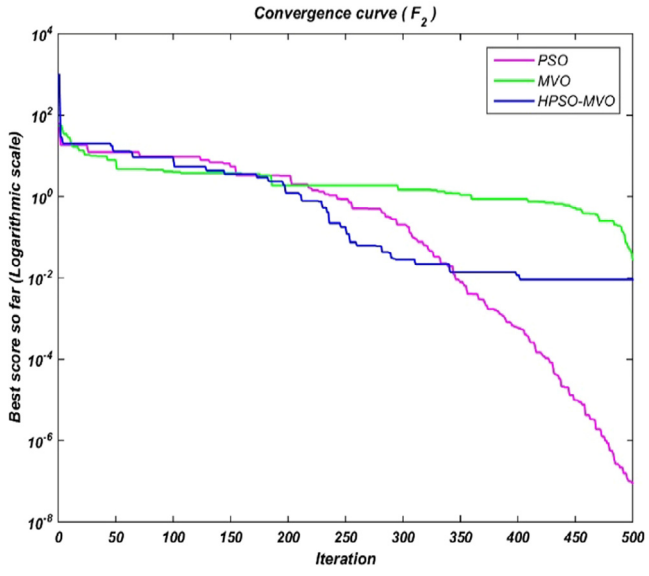

Fig. 3. Convergence curve of function F2.

Please cite this article in press as: P. Jangir et al., A novel hybrid Particle Swarm Optimizer with multi verse optimizer for global numerical optimization and Optimal Reactive Power Dispatch problem, Eng. Sci. Tech., Int. J. (2016), http://dx.doi.org/10.1016/j.jestch.2016.10.007

factor is multiplied by the square of the indifference value of state variables and is included to the objective function and any impractical result achieved is declined [7].

Penalty function may be mathematically formulated as follows:

$$J_{aug} = J + \partial_P (P_{G_1} - P_{G_1}^{lim})^2 + \partial_V \sum_{i=1}^{NLB} (V_{L_i} - V_{L_i}^{lim})^2 + \partial_Q \sum_{i=1}^{NGen} + \partial_S \sum_{i=0}^{Nline} (S_{l_i} - S_{l_i}^{max})^2 \quad (26)$$

where,

$\partial_P, \partial_V, \partial_Q, \partial_S$ = penalty factors
U_{lim} = Boundary value of the state variable U.

If U is greater than the maximum limit, U_{lim} takings the value of this one, if U is lesser than the minimum limit U_{lim} takings the value of that limit. This can be shown as follows [7]:

$$U^{lim} = \begin{cases} U^{upper}; & U > U^{upper} \\ U^{lower}; & U < U^{lower} \end{cases} \quad (27)$$

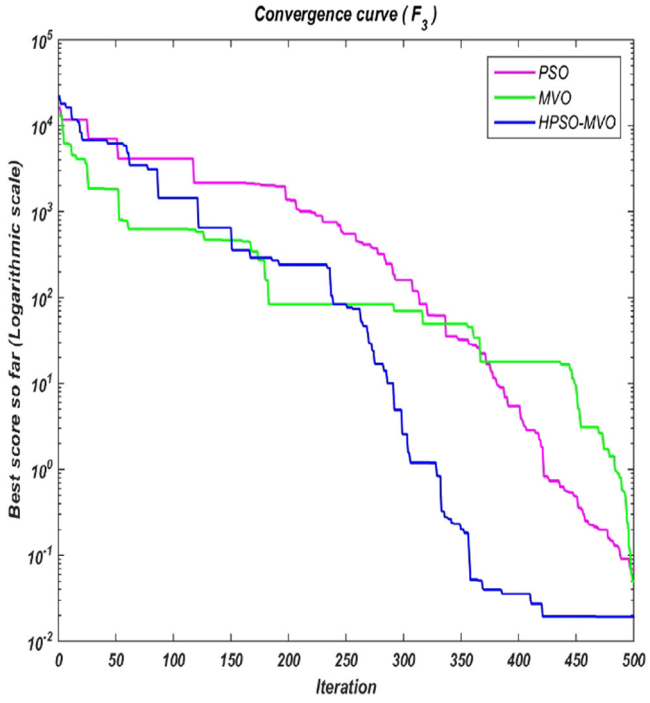

Fig. 4. Convergence curve of function F3.

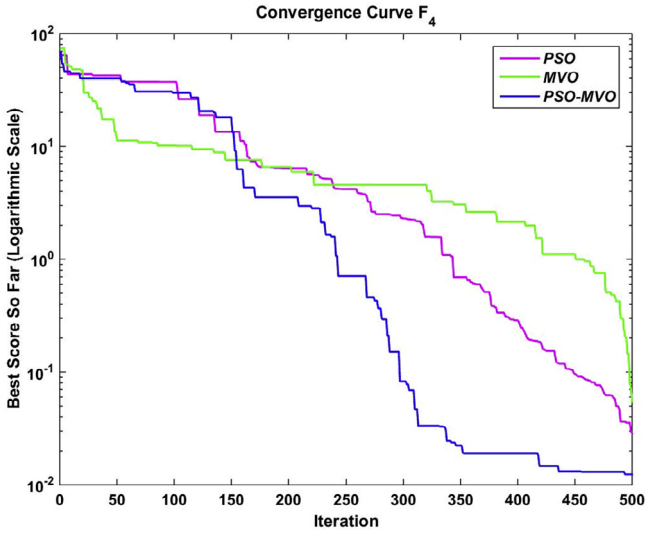

Fig. 5. Convergence curve of function F4.

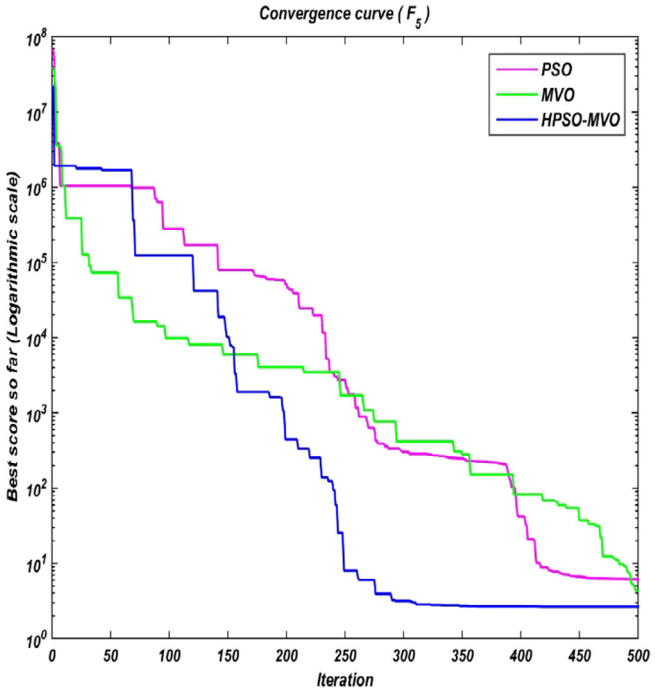

Fig. 6. Convergence curve of function F5.

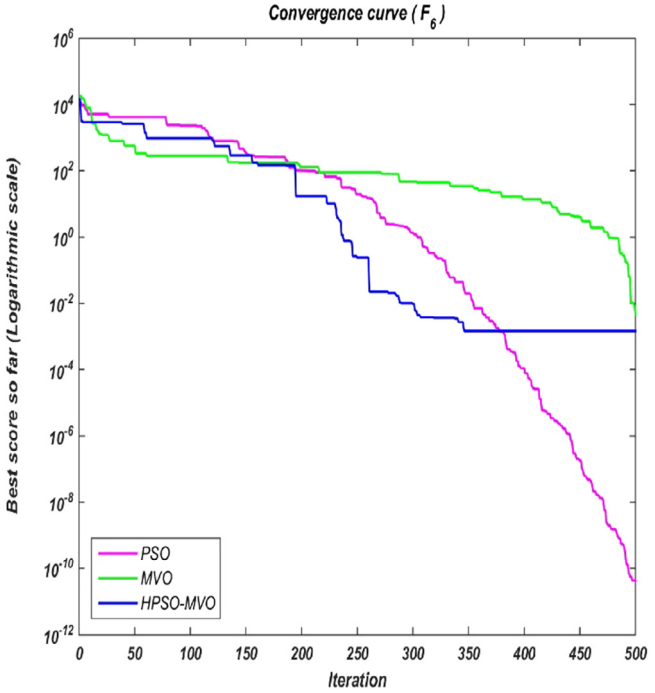

Fig. 7. Convergence curve of function F6.

5. Application and results

The PSO-MVO technique has been implemented for Unconstraint slandered Unimodal, Multimodal, composite function and the ORPD solution for standard IEEE 30-bus test system and for a number of cases with dissimilar objective functions. The used software program is written in MATLAB R2014b computing surroundings and used on a 2.60 GHz i5 PC with 4 GB RAM.

5.1. Unconstraint Test Benchmark Function

The results Shown in Figs. 2–7 on the unimodal functions show in Table 1 the superior exploitation of HPSO-MVO. The exploration ability of WOA is confirmed by the results shown in Figs. 8–13 on multimodal functions show in Table 2. The results shown in Figs. 14–23 on Fixed dimension multi-modal benchmark functions show in Table 3 confirm the performance of WOA in practice and internal parameter of algorithm that shown in Table 4.

In Tables 5–7 represent results of HPSO-MVO, PSO and MVO in terms of Average value, best value and slandered deviation values on Uni-model, multi-model and Fixed dimension multi-modal benchmark functions and Results of Hybrid PSO-MVO Algorithm Best compare to PSO and MVO Algorithms in terms of Average value, best value and slandered deviation values.

Table 1
Uni-modal benchmark functions.

Function	Dim	Range	F_{min}
$f_1(x) = \sum_{i=1}^{n} x_i^2 * R(x)$	10	[−100,100]	0
$f_2(x) = \sum_{i=1}^{n} \lvert x_i \rvert + \prod_{i=1}^{n} \lvert x_i \rvert * R(x)$	10	[−10,10]	0
$f_3(x) = \sum_{i=1}^{n} \left(\sum_{j-1}^{i} x_j \right)^2 * R(x)$	10	[−100,100]	0
$f_4(x) = \max_i \{ \lvert x_i \rvert, 1 \leqslant i \leqslant n \}$	10	[−100,100]	0
$f_5(x) = \sum_{i=1}^{n-1} [100(x_{i+1} - x_i^2)^2 + (x_i - 1)^2] * R(x)$	10	[−30,30]	0
$f_6(x) = \sum_{i=1}^{n} ([x_i + 0.5])^2 * R(x)$	10	[−100,100]	0
$f_7(x) = \sum_{i=1}^{n} i x_i^4 + random[0,1) * R(x)$	10	[−1.28,1.28]	0

5.2. IEEE 30-bus test system

With the purpose of elucidate the strength of the suggested PSO-MVO technique, it has been verified on the standard IEEE 30-bus test system as displays in Fig. 24. The standard IEEE 30-bus test system shown in Fig. 24 selected in this work has the following features [7,12]: six generating units at buses 1,2,5,8,11 and

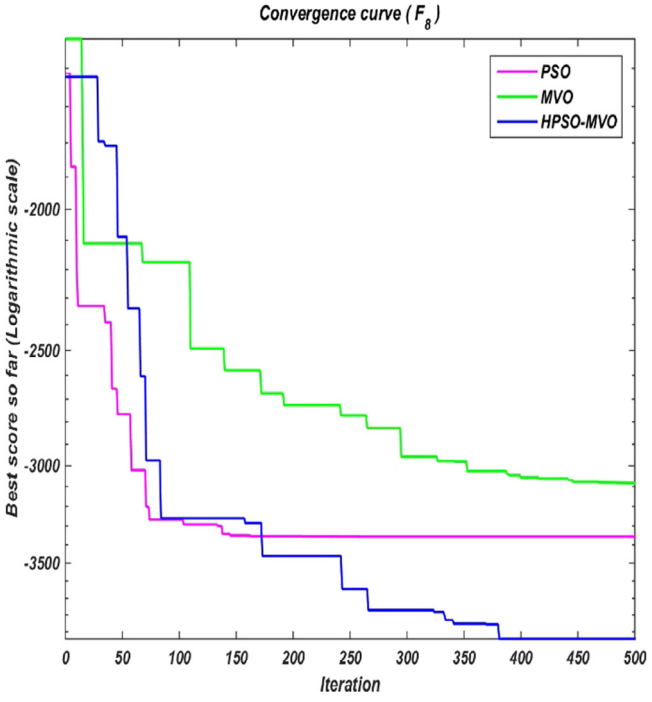

Fig. 9. Convergence curve of function F8.

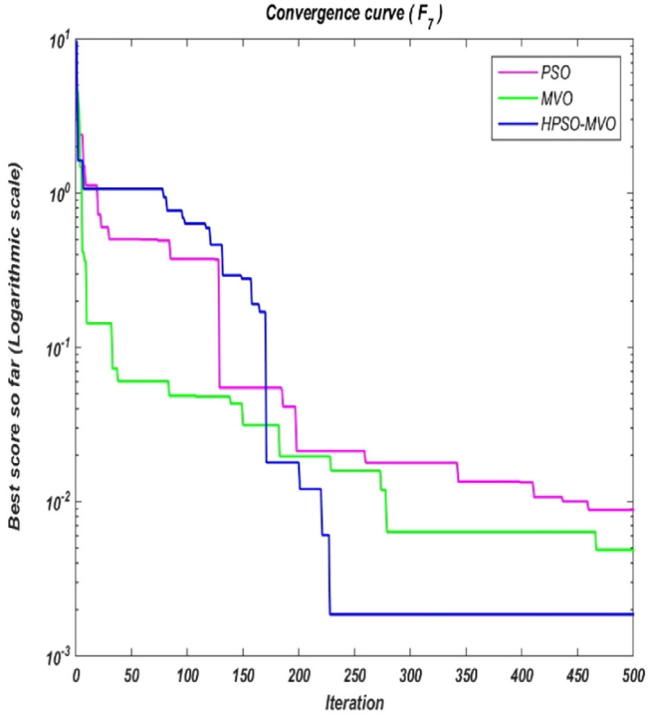

Fig. 8. Convergence curve of function F7.

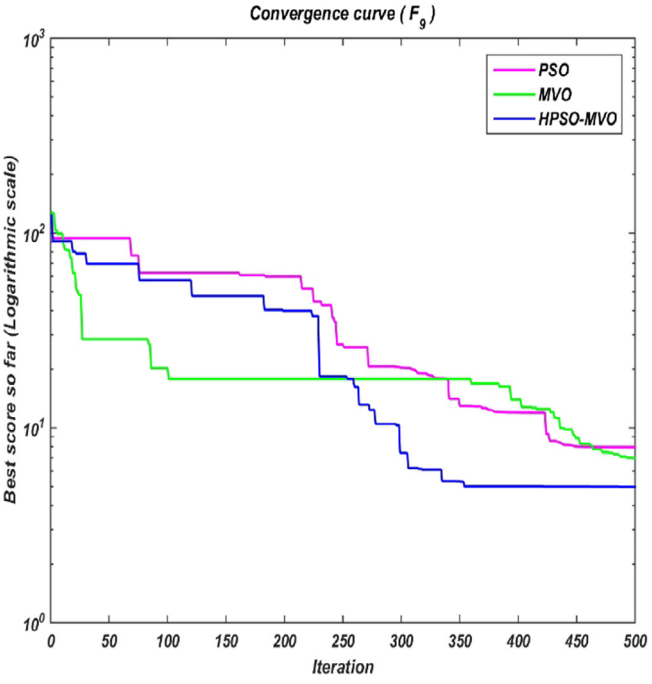

Fig. 10. Convergence curve of function F9.

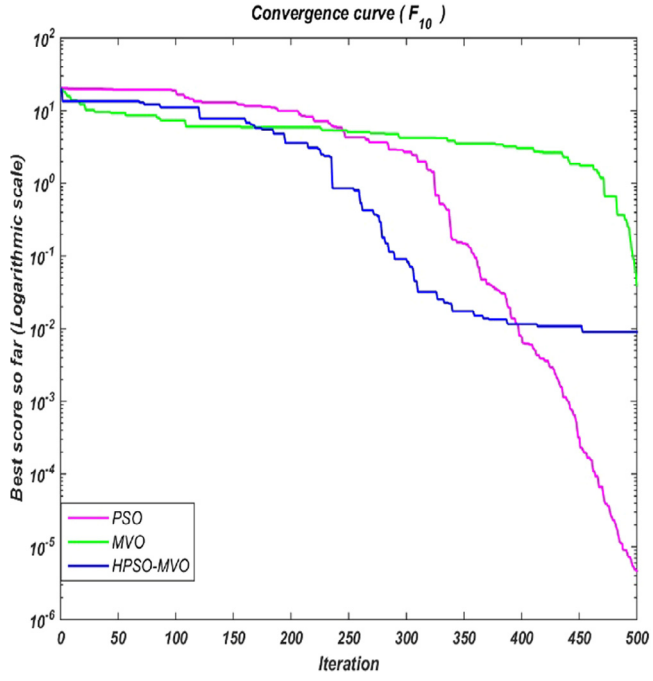

Fig. 11. Convergence curve of function F10.

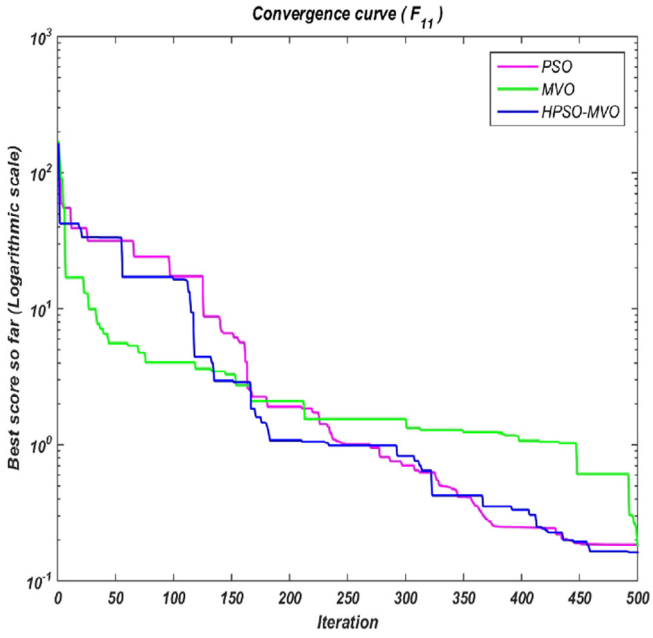

Fig. 12. Convergence curve of function F11.

13, four regulating transformers having off-nominal tap ratio between buses 4–12, 6–9, 6–10 and 28–27 and nine shunt VAR compensators at buses 10,12,15,17,20,21,23,24 and 29.

In addition, generator cost coefficient data, the line data, bus data, and the upper and lower bounds for the control variables are specified in [12].

In given test system, five diverse cases have been considered with various purposes and all the acquired outcomes are given in Tables 3, 5, 7, 9 and 11. The very first column of this tables denotes the optimal values of control variables found where (see Figs. 25 and 29):

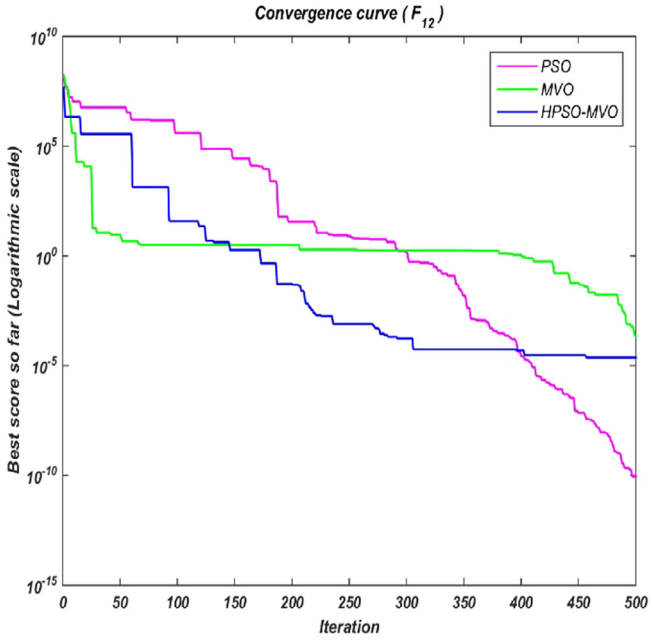

Fig. 13. Convergence curve of function F12.

- P_{G1} through P_{G6} and V_{G1} through V_{G6} signifies the power and voltages of generator 1 to generator 6.
- T_{4-12}, T_{6-9}, T_{6-10} and T_{28-27} are the transformer tap settings comprised between buses 4–12, 6–9, 6–10 and 28–27.
- Q_{C10}, Q_{C12}, Q_{C15}, Q_{C17}, Q_{C20}, Q_{C21}, Q_{C23}, Q_{C24} and Q_{C29} denote the shunt VAR compensators coupled at buses 10, 12, 15, 17, 20, 21, 23, 24 and 29.

Further, fuel cost (*$/h*), real power losses (*MW*), reactive power losses (*MVAR*), voltage deviation and *Lmax* represent the total generation fuel cost of the system, the total real power losses, the total reactive power losses, the load voltages deviation from 1 and the stability index, respectively. Other particulars for these outcomes will be specified in the next sections.

The control parameters for PSO-MVO, MVO, PSO used in this problem are given in the Table 8.

5.2.1. Case 1: Minimization of generation fuel cost.

The very common ORPD objective that is generation fuel cost reduction shown in Fig. 3 is considered in the case 1. Therefore, the objective function Y indicates the complete fuel cost of total generating units and it is calculated by following equation [1]:

$$Y = \sum_{i=1}^{NGen} f_i(\$/h) \tag{28}$$

where, f_i is the total fuel cost of ith generator, f_i, may be formulated as follow:

$$f_i = u_i + v_i P_{Gi} + w_i P_{Gi}^2 (\$/h) \tag{29}$$

where, u_i, v_i and w_i are the simple, the linear and the quadratic cost coefficients of the ith generator, respectively. The cost coefficients values are specified in [12].

The variation of the total fuel cost with different algorithms over iterations is presented in Fig. 24. It demonstrates that the suggested method has outstanding convergence characteristics. The comparison of fuel cost obtained with different methods are shown in Table 9 which displays that the results obtained by PSO-MVO is better than the other methods. The optimal values of control

Table 2
Multi-modal benchmark functions.

Function	Dim	Range	F_{min}
$F_8(x)=\sum_{i=1}^{n}-x_i sin(\sqrt{\lvert x_i\rvert})*R(x)$	10	[−500,500]	(−418.9829*5)
$F_9(x)=\sum_{i=1}^{n}[x_i^2-10cos(2\pi x_i)+10]*R(x)$	10	[−5.12,5.12]	0
$F_{10}(x)=-20exp\left(-0.2\sqrt{\frac{1}{n}\sum_{i=1}^{n}x_i^2}\right)-exp(\frac{1}{n}\sum_{i=1}^{n}cos(2\pi x_i))+20+e*R(x)$	10	[−32,32]	0
$F_{11}(x)=\frac{1}{4000}\sum_{i=1}^{n}x_i^2-\prod_{i=1}^{n}cos\left(\frac{x_i}{\sqrt{i}}\right)+1*R(x)$	10	[−600,600]	0
$F_{12}(x)=\frac{\pi}{n}\left\{\begin{matrix}10sin(\pi y_1)+\sum_{i=1}^{n-1}(y_i-1)^2\\ [1+10sin^2(\pi y_{i+1})]+(y_n-1)^2\end{matrix}\right\}y_i=1+\frac{x_i+1}{4},$ $u(x_i,a,k,m)=\left\{\begin{matrix}k(x_i-a)^m x_i>a\\ 0-a<x_i<a\\ k(-x_i-a)^m x_i<-a\end{matrix}\right.$	10	[−50,50]	0
$F_{13}(x)=0.1\left\{\begin{matrix}sin^2(3\pi x_1)+\sum_{i=1}^{n}(x_i-1)^2[1+sin^2(3\pi x_i+1)]\\ +(x_n-1)^2[1+sin^2(2\pi x_n)]\end{matrix}\right\}+\sum_{i=1}^{n}u(x_i,5,100,4)*R(x)$	10	[−50,50]	0

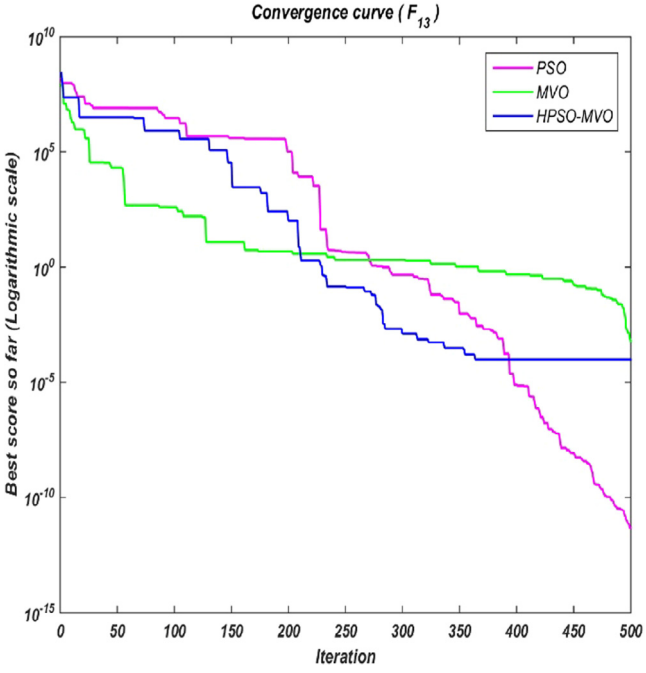

Fig. 14. Convergence curve of function F13.

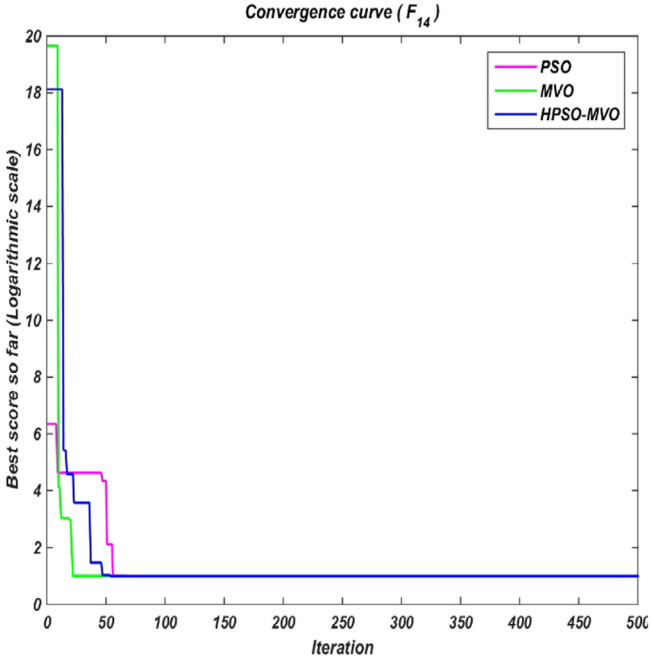

Fig. 15. Convergence curve of function F14.

variables obtained by different algorithms for case 1 are specified in Table 10. By means of the same settings i.e. control variables boundaries, initial conditions and system data, the results achieved in case 1 with the PSO-MVO technique are compared to some other methods and it displays that the total fuel cost is greatly reduced compared to the initial case [7]. Quantitatively, it is reduced from 901.951$/h to 799.101$/hr.

5.2.2. Case 2: Voltage profile improvement.

Bus voltage is considered as most essential and important security and service excellence indices [7]. Here the goal is to reduce the fuel cost and increase voltage profile simultaneously by reducing the voltage deviation of *PQ* (*load*) buses from the unity 1.0 *p.u.*

Hence, the objective function may be formulated by following equation [5]:

$$Y = Y_{cost} + wY_{voltage-deviation} \tag{30}$$

where, w is an appropriate weighting factor, to be chosen by the user to offer a weight or importance to each one of the two terms of the objective function. Y_{cost} and $Y_{voltage-deviation}$ are specified as follows [5]:

$$Y_{cost} = \sum_{i=1}^{NGen} f_i \tag{31}$$

$$Y_{voltage\_deviation} = \sum_{i=1}^{NGen} |V_i - 1.0| \tag{32}$$

The variation of voltage deviation shown in Fig. 26 with different algorithms over iterations is sketched in Fig. 3. It demonstrates that the suggested method has good convergence characteristics. The statistical values of voltage deviation obtained with different methods are shown in Table 18 which displays that the results obtained by PSO-MVO is better than the other methods. The optimal values of control variables obtained by different algorithms for case 2 are specified in Table 12. By means of the same settings the results achieved in case 2 with the PSO-MVO technique are compared to some other methods and it displays that the voltage

Please cite this article in press as: P. Jangir et al., A novel hybrid Particle Swarm Optimizer with multi verse optimizer for global numerical optimization and Optimal Reactive Power Dispatch problem, Eng. Sci. Tech., Int. J. (2016), http://dx.doi.org/10.1016/j.jestch.2016.10.007

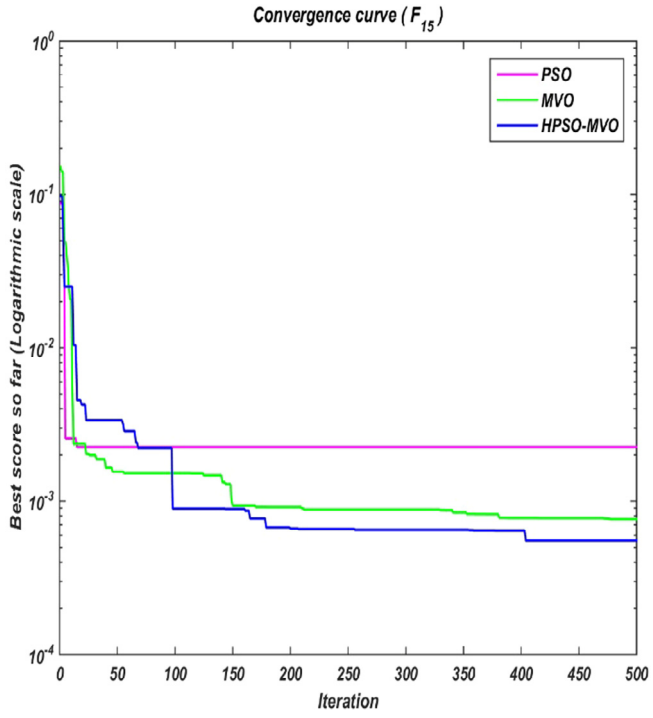

Fig. 16. Convergence curve of function F15.

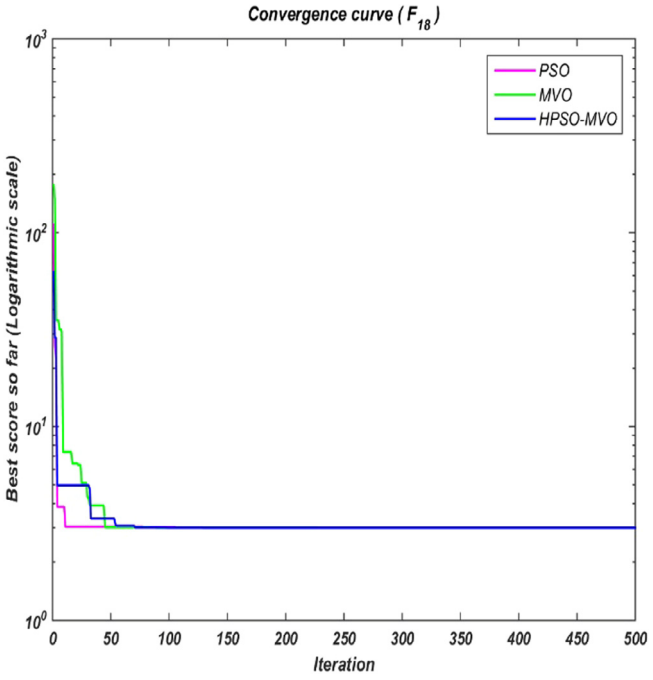

Fig. 18. Convergence curve of function F18.

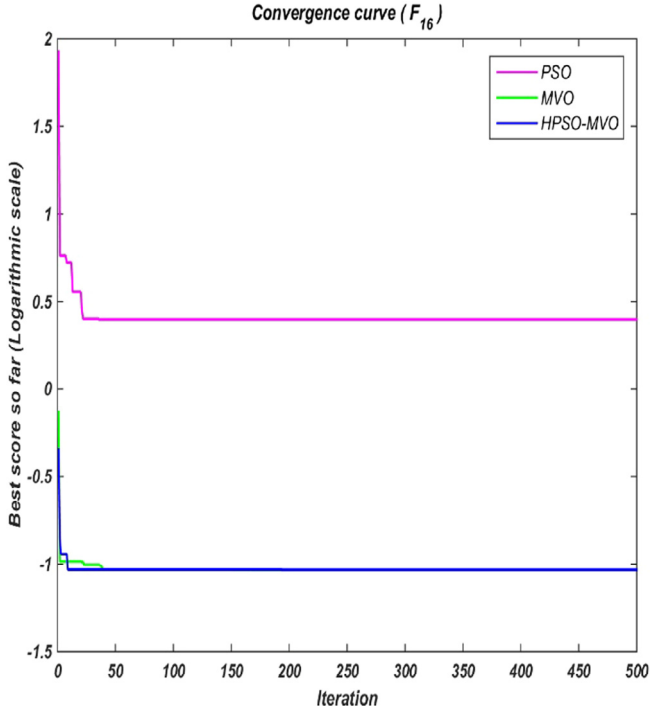

Fig. 17. Convergence curve of function F16.

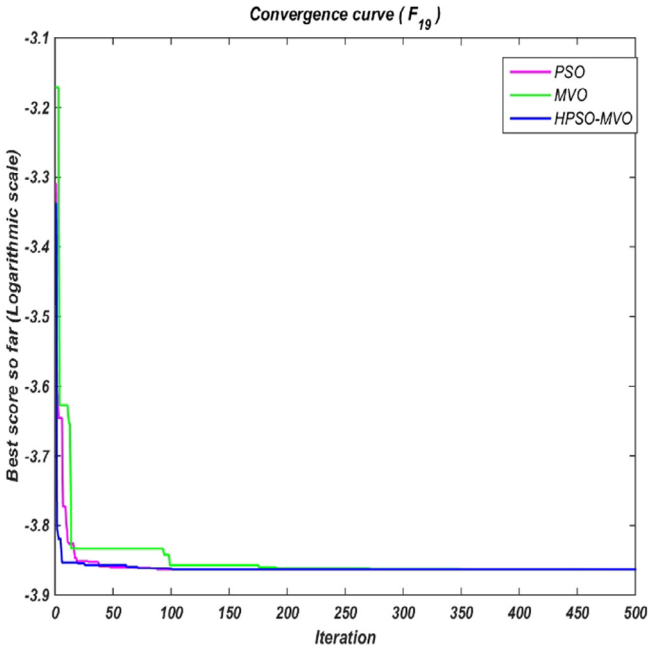

Fig. 19. Convergence curve of function F19.

deviation is greatly reduced compared to the initial case [7]. It has been made known that the voltage deviation is reduced from 1.1496 p.u. to 0.0994 p.u. using PSO-MVO technique.

5.2.3. Case 3: Voltage stability enhancement

Presently, the transmission systems are enforced to work nearby their safety bounds, because of cost-effective and environmental causes. One of the significant characteristic of the system is its capability to retain continuously tolerable bus voltages to each node beneath standard operational environments, next to the rise in load, as soon as the system is being affected by disturbance. The unoptimized control variables may cause increasing and unmanageable voltage drop causing a tremendous voltage collapse [5]. Hence, voltage stability is inviting ever more attention. By using various techniques to evaluate the margin of voltage stability, Glavitch and Kessel have introduced a voltage stability index called L-index depends on the viability of load flow equations for every

Please cite this article in press as: P. Jangir et al., A novel hybrid Particle Swarm Optimizer with multi verse optimizer for global numerical optimization and Optimal Reactive Power Dispatch problem, Eng. Sci. Tech., Int. J. (2016), http://dx.doi.org/10.1016/j.jestch.2016.10.007

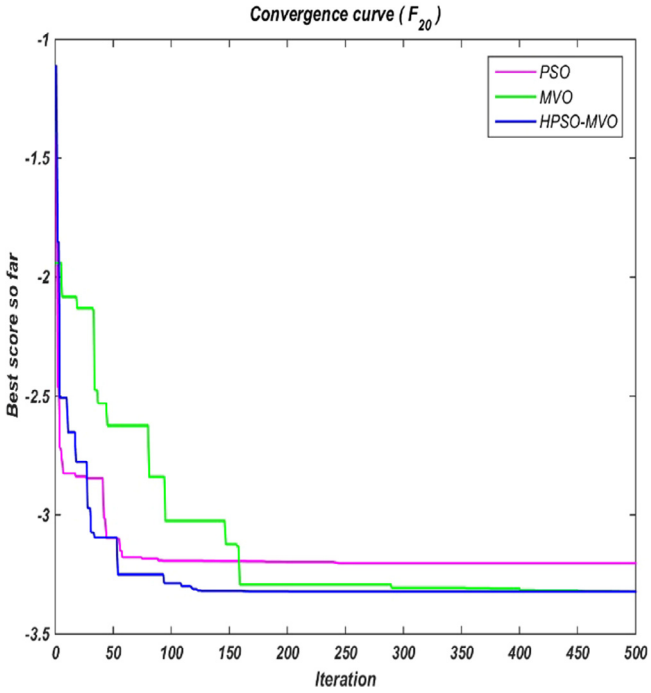

Fig. 20. Convergence curve of function F20.

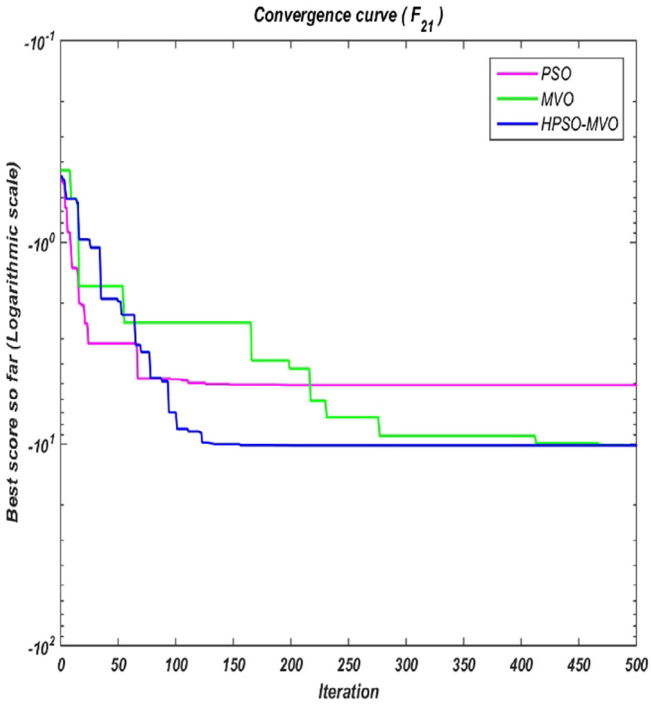

Fig. 21. Convergence curve of function F21.

node [14]. The L-index of a bus shows the probability of voltage collapse circumstance for that particular bus. It differs between 0 and 1 equivalent to zero load and voltage collapse, respectively.

For the given system with *NB, NGen* and *NLB* buses signifying the total No. of buses, the total No. of generator buses and the total No. of load buses, respectively. The buses can be distinct as *PV* (*generator*) buses at the head and *PQ* (*load*) buses at the tail as follows [5]:

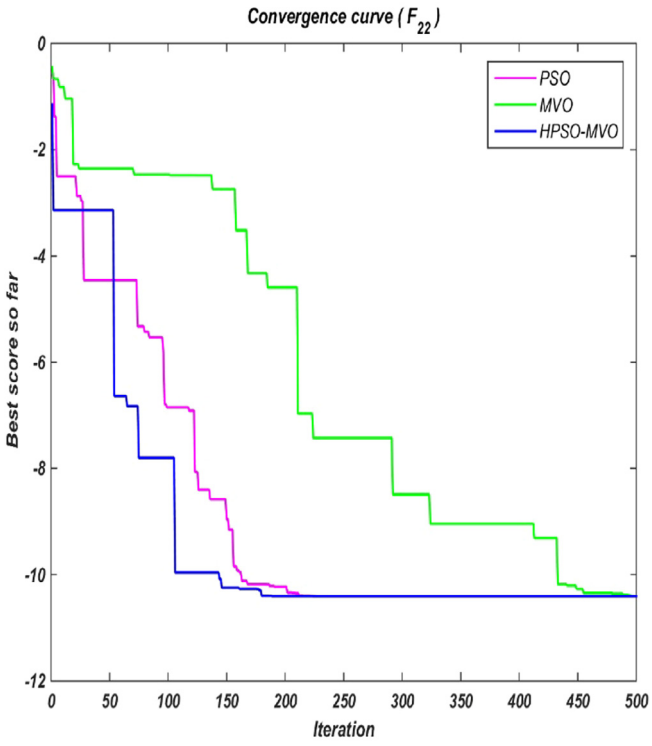

Fig. 22. Convergence curve of function F22.

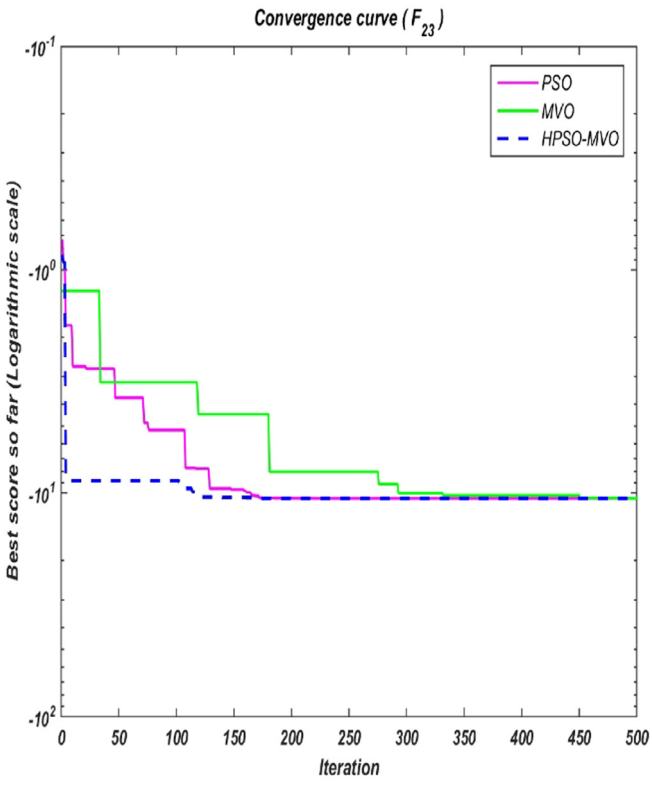

Fig. 23. Convergence curve of function F23.

$$\begin{bmatrix} I_L \\ I_G \end{bmatrix} = [Y_{bus}] \begin{bmatrix} V_L \\ V_G \end{bmatrix} = \begin{bmatrix} Y_{LL} & Y_{LG} \\ Y_{GL} & Y_{GG} \end{bmatrix} \begin{bmatrix} V_L \\ V_G \end{bmatrix} \quad (33)$$

Please cite this article in press as: P. Jangir et al., A novel hybrid Particle Swarm Optimizer with multi verse optimizer for global numerical optimization and Optimal Reactive Power Dispatch problem, Eng. Sci. Tech., Int. J. (2016), http://dx.doi.org/10.1016/j.jestch.2016.10.007

Table 3
Fixed dimension multi-modal benchmark functions.

Function	Dim	Range	F_{min}
$F_{14}(x)=\left(\frac{1}{500}+\sum_{j=1}^{25}\frac{1}{j+\sum_{i=1}^{2}(x_i-a_{ij})^6}\right)^{-1}$	2	[−65.536,65.536]	1
$f_{15}(x)=\sum_{i=1}^{11}a_i-\left[\frac{x_1(b_i^2+b_ix_2)}{b_i^2+b_ix_3+x_4}\right]^2$	4	[−5,5]	0.00030
$f_{16}(x)=4x_1^2-2.1x_1^4+\frac{1}{3}x_1^6+x_1x_2-4x_2^2+4x_2^4$	2	[−5,5]	−1.0316
$f_{17}(x)=\left(x_2-\frac{5.1}{4\pi^2}x_1^2+\frac{5}{\pi}x_1-6\right)^2+10\left(1-\frac{1}{8\pi}\right)\cos x_1+10$	2	[−5,0] [10,15]	0.398
$f_{18}(x)=\left[\begin{array}{c}1+(x_1+x_2+1)^2\\ \left(\begin{array}{c}19-14x_1+3x_1^2-\\ 14x_2+6x_1x_2+3x_2^2\end{array}\right)\end{array}\right]*\left[\begin{array}{c}30+(2x_1-3x_2)^2\\ *\left(\begin{array}{c}18-32x_1+12x_1^2+\\ 48x_2-36x_1x_2+27x_2^2\end{array}\right)\end{array}\right]$	2	[−2,2]	3
$f_{19}(x)=-\sum_{i=1}^{4}c_i\exp\left(-\sum_{j=1}^{3}a_{ij}(x_j-p_{ij})^2\right)$	3	[0,1]	−3.86
$f_{20}(x)=-\sum_{i=1}^{4}c_i\exp\left(-\sum_{j=1}^{6}a_{ij}(x_j-p_{ij})^2\right)$	6	[0,1]	−3.32
$f_{21}(x)=-\sum_{i=1}^{5}[(X-a_i)(X-a_i)^T+c_i]^{-1}$	4	[0,10]	−10.1532
$f_{22}(x)=-\sum_{i=1}^{7}[(X-a_i)(X-a_i)^T+c_i]^{-1}$	4	[0,10]	−10.4028
$f_{23}(x)=-\sum_{i=1}^{10}[(X-a_i)(X-a_i)^T+c_i]^{-1}$	4	[0,10]	−10.5363

Table 4
Internal Parameters.

Parameter Name	Search Agents No.	Max. Iteration No.	No. of Evolution
F1-F23	30	500	5–20

Note: Scale specified on axis, Not specified means axis are linear scale.

Table 5
Result for Uni-modal benchmark functions.

Fun.	Std. PSO			Std. MVO			HPSO-MVO		
	Ave	Best	S.D.	Ave	Best	S.D.	Ave	Best	S.D.
F1	7.687E−11	**7.553E−11**	1.88E−12	0.0087	0.0083	6.6060E−04	5.4729E−04	2.5304E−04	4.1613E−04
F2	2.416E−07	**9.005E−08**	2.144E−07	0.0339	0.0284	0.0077	0.0156	0.0090	0.0093
F3	0.1510	0.6918	0.1157	0.0715	0.0494	0.0312	0.0252	**0.0193**	0.0083
F4	0.0340	0.0287	0.0075	0.0557	0.0544	0.0018	0.0216	**0.0124**	0.0130
F5	118.57	6.1391	159.01	52.5296	4.2602	68.2633	5.2500	**2.6575**	3.6663
F6	8.7470E−10	**4.1227E−11**	1.1787E−09	0.0067	0.0047	0.0028	0.0029	0.0015	0.0020
F7	0.0095	0.0088	0.001	0.0092	0.0049	0.0061	0.0029	**0.0019**	0.0015

The significance of bold text represent best value of fitness function in the table.

Table 6
Result for multi-modal benchmark functions.

Fun.	Std. PSO			Std. MVO			HPSO-MVO		
	Ave	Best	S.D.	Ave	Best	S.D.	Ave	Best	S.D.
F8	−3.29E+03	−3.35E+03	84.8	−2.73E+03	−3.08E+03	489.4	−3.61E+03	**−3.94E+03**	459.00
F9	8.0765	7.9597	0.16	11.450	6.9745	6.329	7.4680	**4.9832**	3.5141
F10	6.2788E−06	**4.6271E−06**	2.33E−06	0.0473	0.0397	0.010	0.0159	0.0090	0.0098
F11	0.1970	0.1847	0.01	0.5599	0.1827	0.533	0.2376	**0.1622**	0.1066
F12	1.155E−10	**9.136E−11**	3.42E−11	9.029E−04	2.249E−04	9.588E−04	0.0063	2.339E−05	0.0089
F13	6.756E−12	**4.996E−12**	2.48E−12	0.0028	6.091E−04	0.003	1.472E−04	9.962E−05	6.7358E−05

The significance of bold text represent best value of fitness function in the table.

Table 7
Result for Fixed dimension multi-modal benchmark functions.

Fun.	Std. PSO			Std. MVO			HPSO-MVO		
	Ave	Best	S.D.	Ave	Best	S.D.	Ave	Best	S.D.
F14	0.9980	**0.9980**	0	0.9980	**0.9980**	6.51E−11	0.9980	**0.9980**	1.14E−14
F15	0.0124	0.0023	0.0144	9.9363E−04	7.6374E−04	3.25E−04	6.4613E−04	**5.5411E−04**	1.30E−04
F16	−1.031	**−1.0316**	2.2E−16	−1.0316	**−1.0316**	2.00E−07	−1.0316	**−1.0316**	1.86E−11
F17	0.397	0.3979	0	N/A	N/A	N/A	N/A	N/A	N/A
F18	3.0000	**3.0000**	1.8E−15	3.0000	**3.0000**	3.64E−06	3.0000	**3.0000**	7.14E−11
F19	−3.862	**−3.8628**	4.4E−16	−3.8628	**−3.8628**	3.05E−07	−3.8628	**−3.8628**	8.37E−11
F20	−3.201	−3.2031	0.0025	−3.2591	**−3.3220**	0.0889	−3.2350	**−3.3220**	0.1231
F21	−3.891	−5.1008	1.7097	−6.3916	−10.1528	5.3191	−7.6270	**−10.153**	3.5726
F22	−10.4029	**−10.4029**	1.7E−15	−7.7450	**−10.4026**	3.7584	−10.4029	**−10.4029**	1.23E−06
F23	−6.479	**−10.5364**	5.7379	−10.536	**−10.5363**	4.34E−04	−10.536	**−10.536**	2.61E−06

The significance of bold text represent best value of fitness function in the table.

Please cite this article in press as: P. Jangir et al., A novel hybrid Particle Swarm Optimizer with multi verse optimizer for global numerical optimization and Optimal Reactive Power Dispatch problem, Eng. Sci. Tech., Int. J. (2016), http://dx.doi.org/10.1016/j.jestch.2016.10.007

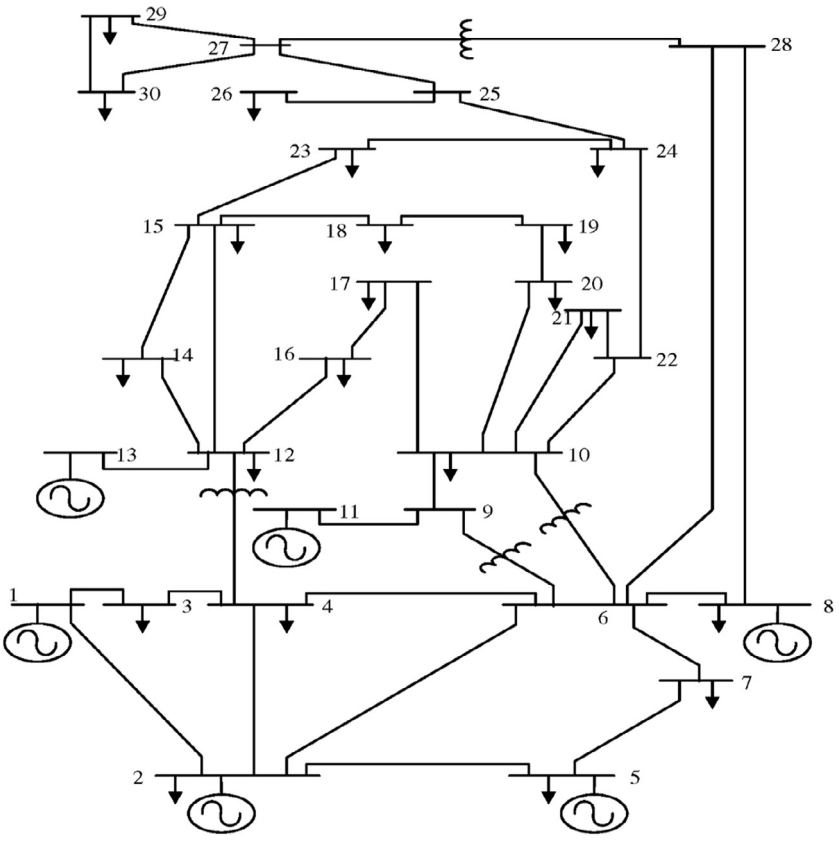

Fig. 24. Single line diagram of IEEE 30-bus test system.

Table 8
Basic parameters used in ORPD problem for PSO-MVO, MVO and PSO.

Sr. No.	Parameters	Value
1	Population (No. of Search agents) (N)	40
2	Maximum iterations count (t)	500
3	No. of Variables (dim)	6
4	Random Number	[0,1]

Table 9
Comparison of fuel cost obtained with different algorithms.

Method	Fuel Cost ($/hr)	Method Description
HPSO-MVO	**799.101**	Hybrid Particle Swarm Optimization-Multi Verse Optimizer
MVO	799.242	Multi Verse Optimizer
PSO	799.704	Particle Swarm Optimization
DE	799.289	Differential Evolution [6]
BHBO	799.921	Black Hole- Based Optimization [7]

The significance of bold text represent best value of fitness function in the table.

where, Y_{LL}, Y_{LG}, Y_{GL} and Y_{GG} are co-matrix of Y_{bus}. The subsequent hybrid system of equations can be expressed as:

$$\begin{bmatrix} V_L \\ I_G \end{bmatrix} = [H] \begin{bmatrix} I_L \\ V_G \end{bmatrix} = \begin{bmatrix} H_{LL} & H_{LG} \\ H_{GL} & H_{GG} \end{bmatrix} \begin{bmatrix} I_L \\ V_G \end{bmatrix} \tag{34}$$

where matrix H is produced by the partially inversing of Y_{bus}, H_{LL}, H_{LG}, H_{GL} and H_{GG} are co- matrix of H, V_G, I_G, V_L and I_L are voltage and current vector of Generator buses and load buses, respectively.

The matrix H is given by:

Table 10
Optimal values of control variables for case 1 with different algorithms.

Control Variable	Min	Max	Initial	PSO-MVO	MVO	PSO
P_{G1}	50	200	99.2230	177.104	177.349	177.105
P_{G2}	20	80	80	48.645	48.712	48.748
P_{G5}	15	50	50	21.261	21.278	21.318
P_{G8}	10	35	20	21.060	20.962	20.986
P_{G11}	10	30	20	11.966	11.836	12.049
P_{G13}	12	40	20	12.000	12.000	12.000
V_{G1}	0.95	1.1	1.05	1.100	1.100	1.100
V_{G2}	0.95	1.1	1.04	1.088	1.088	1.088
V_{G5}	0.95	1.1	1.01	1.061	1.061	1.061
V_{G8}	0.95	1.1	1.01	1.069	1.070	1.070
V_{G11}	0.95	1.1	1.05	1.100	1.100	1.100
V_{G13}	0.95	1.1	1.05	1.100	1.100	1.100
$T_{4\text{-}12}$	0	1.1	1.078	1.021	0.964	0.976
$T_{6\text{-}9}$	0	1.1	1.069	0.913	1.045	0.975
$T_{6\text{-}10}$	0	1.1	1.032	0.995	1.038	1.015
$T_{28\text{-}27}$	0	1.1	1.068	0.971	0.990	0.966
QC_{10}	0	5	0	1.595	3.525	2.353
QC_{12}	0	5	0	4.929	1.770	5.000
QC_{15}	0	5	0	5.000	2.029	0.000
QC_{17}	0	5	0	5.000	2.028	0.689
QC_{20}	0	5	0	5.000	3.514	0.003
QC_{21}	0	5	0	5.000	2.415	5.000
QC_{23}	0	5	0	4.926	1.551	0.000
QC_{24}	0	5	0	5.000	2.997	0.000
QC_{29}	0	5	0	2.393	3.991	0.000
Fuel Cost($/hr)	–	–	901.951	**799.101**	799.242	799.704

The significance of bold text represent best value of fitness function in the table.

$$[H] = \begin{bmatrix} Z_{LL} & -Z_{LL}Y_{LG} \\ Y_{GL}Z_{LL} & Y_{GG} - Y_{GL}Z_{LL}Y_{LG} \end{bmatrix} Z_{LL} = Y_{LL}^{-1} \tag{35}$$

Hence, the L-index denoted by L_j of bus j is represented as follows:

Please cite this article in press as: P. Jangir et al., A novel hybrid Particle Swarm Optimizer with multi verse optimizer for global numerical optimization and Optimal Reactive Power Dispatch problem, Eng. Sci. Tech., Int. J. (2016), http://dx.doi.org/10.1016/j.jestch.2016.10.007

Table 11
Comparison of voltage deviations obtained with different algorithms.

Method	Voltage deviation (p.u)	Method description
HPSO-MVO	**0.0994**	Hybrid Particle Swarm Optimization-Multi Verse Optimizer
MVO	0.1056	Multi Verse Optimizer
PSO	0.1506	Particle Swarm Optimization
DE	0.1357	Differential Evolution [6]
BHBO	0.1262	Black Hole- Based Optimization [7]

The significance of bold text represent best value of fitness function in the table.

$$L_j = \left| 1 - \sum_{i=1}^{NGen} H_{LG_{ji}} \frac{v_i}{v_j} \right| \quad j = 1, 2 \ldots, NL \tag{36}$$

Hence, the stability of the whole system is described by a global indicator $L_{\max}$ which is given by [7],

$$L_{\max} = \max(L_j) \quad j = 1, 2 \ldots, NL \tag{37}$$

The system is more stable as the value of $L_{\max}$ is lower.

The voltage stability can be enhance by reducing the value of voltage stability indicator *L-index* at every bus of the system [7].

Thus, the objective function may be given as follows:

$$Y = Y_{cost} + wY_{voltage\_Stability\_Enhancement} \tag{38}$$

where,

$$Y_{cost} = \sum_{i=1}^{NGen} f_i \tag{39}$$

$$Y_{voltage\_stability\_enhancement} = L_{\max} \tag{40}$$

The variation of the *Lmax* index with different algorithms over iterations is presented in Fig. 27. The statistical results obtained with different methods are shown in Table 13 which displays that PSO-MVO method gives better results than the other methods. The optimal values of control variables obtained by different algorithms for case 3 are given in Table 14. After applying the PSO-MVO technique, it appears from Table 14 that the value of *Lmax*

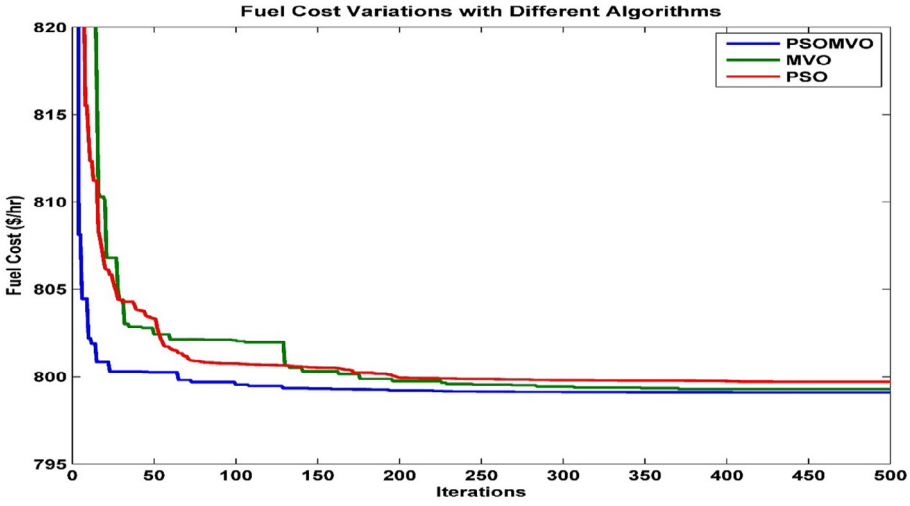

Fig. 25. Fuel cost variations with different algorithms.

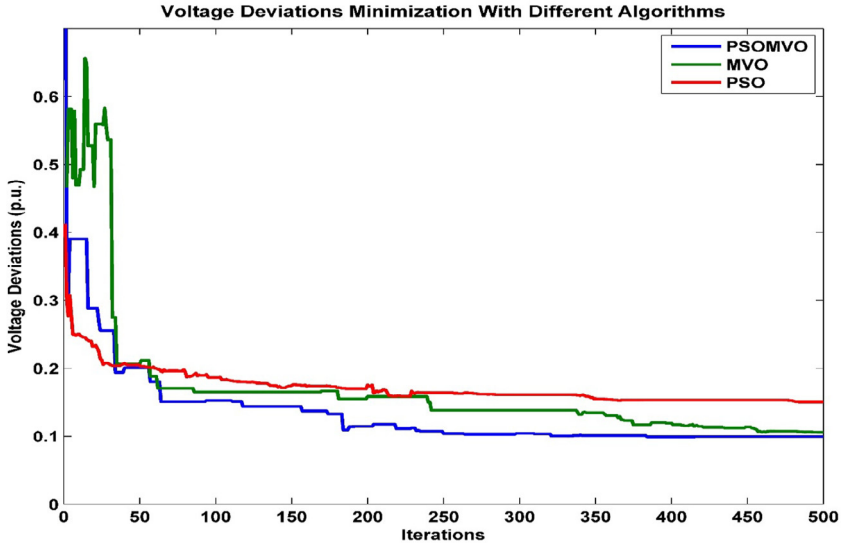

Fig. 26. Voltage deviation minimization with different algorithms.

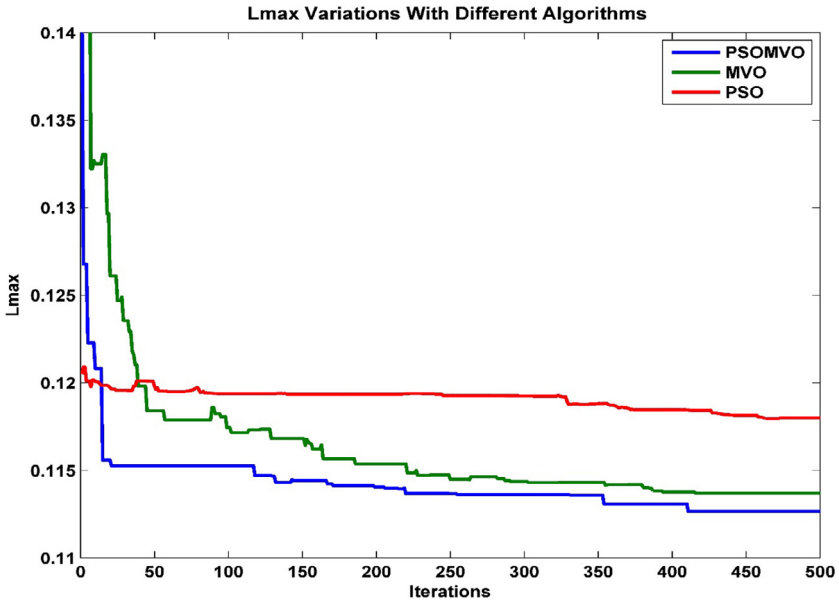

Fig. 27. *Lmax* variations with different algorithms.

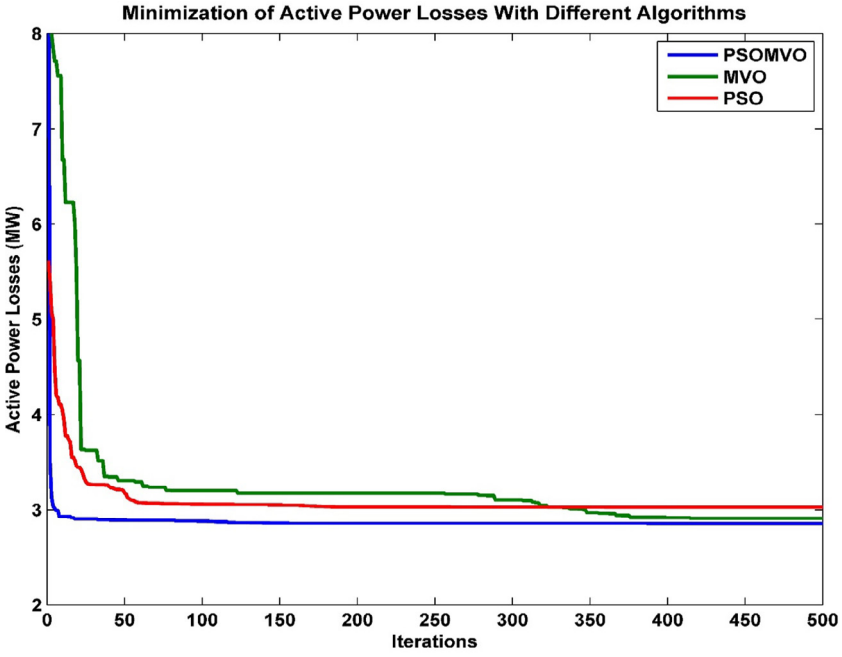

Fig. 28. Minimization of active power losses with different algorithms.

is considerably decreased in this case compared to initial [7] from 0.1723 to 0.1127. Thus, the distance from breakdown point is improved.

5.2.4. Case 4: Minimization of active power transmission losses

In the case 4 the Optimal Reactive Power Dispatch objective is to reduce the active power transmission losses, which can be represented by power balance equation as follows [7]:

$$J = \sum_{i=1}^{NGen} P_i = \sum_{i=1}^{NGen} P_{Gi} - \sum_{i=1}^{NGen} P_{Di} \quad (41)$$

Fig. 27 shows the tendency for reducing the total real power losses objective function using the different techniques. The active power losses obtained with different techniques are shown in Table 15 which made sense that the results obtained by PSO-MVO gives better values than the other methods. The optimal values of control variables obtained by different algorithms for case 4 shown in Fig. 28 are displayed in Table 16. By means of the same settings the results achieved in case 4 with the PSO-MVO technique are compared to some other methods and it displays that the real power transmission losses are greatly reduced compared to the initial case [7] from 5.821 to 2.854.

Please cite this article in press as: P. Jangir et al., A novel hybrid Particle Swarm Optimizer with multi verse optimizer for global numerical optimization and Optimal Reactive Power Dispatch problem, Eng. Sci. Tech., Int. J. (2016), http://dx.doi.org/10.1016/j.jestch.2016.10.007

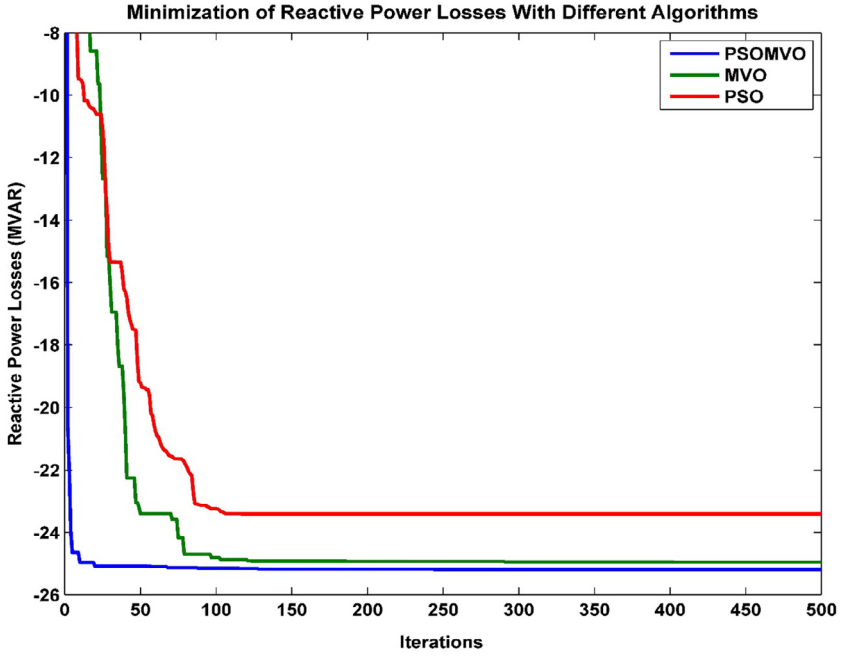

Fig. 29. Minimization of reactive power transmission losses with different algorithms.

Table 12
Optimal values of control variables for case 2 with different algorithms.

Control Variable	Min	Max	Initial	PSO-MVO	MVO	PSO
P_{G1}	50	200	99.2230	176.258	177.983	175.922
P_{G2}	20	80	80	49.011	48.765	46.389
P_{G5}	15	50	50	21.857	21.475	21.597
P_{G8}	10	35	20	21.314	20.158	19.396
P_{G11}	10	30	20	12.816	12.932	17.656
P_{G13}	12	40	20	12.008	12.029	12.000
V_{G1}	0.95	1.1	1.05	1.038	1.045	1.047
V_{G2}	0.95	1.1	1.04	1.023	1.027	1.034
V_{G5}	0.95	1.1	1.01	1.012	1.010	0.999
V_{G8}	0.95	1.1	1.01	1.003	1.004	1.005
V_{G11}	0.95	1.1	1.05	1.062	1.065	0.999
V_{G13}	0.95	1.1	1.05	0.988	0.996	1.018
$T_{4\text{-}12}$	0	1.1	1.078	1.083	1.077	0.954
$T_{6\text{-}9}$	0	1.1	1.069	0.900	0.900	0.969
$T_{6\text{-}10}$	0	1.1	1.032	0.946	0.928	0.989
$T_{28\text{-}27}$	0	1.1	1.068	0.958	0.965	0.960
QC_{10}	0	5	0	4.202	4.973	3.948
QC_{12}	0	5	0	4.171	0.716	1.765
QC_{15}	0	5	0	4.659	0.382	4.844
QC_{17}	0	5	0	0.000	0.434	3.075
QC_{20}	0	5	0	5.000	3.092	4.687
QC_{21}	0	5	0	5.000	4.398	4.948
QC_{23}	0	5	0	4.692	5.000	1.623
QC_{24}	0	5	0	5.000	3.000	3.559
QC_{29}	0	5	0	1.269	2.234	2.034
Vd	–	–	1.1496	**0.0994**	0.1056	0.1506

The significance of bold text represent best value of fitness function in the table.

Table 13
Comparison of *Lmax* index obtained with different algorithms.

Method	L_{max}	Method description
HPSO-MVO	**0.1127**	Hybrid Particle Swarm Optimization-Multi Verse Optimizer
MVO	0.1136	Multi Verse Optimizer
PSO	0.1180	Particle Swarm Optimization
DE	0.1219	Differential Evolution [6]
BHBO	0.1167	Black Hole- Based Optimization [7]

The significance of bold text represent best value of fitness function in the table.

Table 14
Optimal values of control variables for case 3 with different algorithms.

Control Variable	Min	Max	Initial	PSO-MVO	MVO	PSO
P_{G1}	50	200	99.2230	170.253	180.832	158.331
P_{G2}	20	80	80	46.396	46.817	49.050
P_{G5}	15	50	50	21.281	22.584	18.956
P_{G8}	10	35	20	22.471	15.043	31.224
P_{G11}	10	30	20	19.365	12.948	15.906
P_{G13}	12	40	20	12.075	14.144	17.801
V_{G1}	0.95	1.1	1.05	1.100	1.100	1.098
V_{G2}	0.95	1.1	1.04	1.086	1.089	1.090
V_{G5}	0.95	1.1	1.01	1.085	1.071	1.043
V_{G8}	0.95	1.1	1.01	1.100	1.076	1.058
V_{G11}	0.95	1.1	1.05	1.100	1.083	1.081
V_{G13}	0.95	1.1	1.05	1.100	1.098	1.100
$T_{4\text{-}12}$	0	1.1	1.078	1.070	0.941	0.900
$T_{6\text{-}9}$	0	1.1	1.069	0.961	0.967	1.007
$T_{6\text{-}10}$	0	1.1	1.032	0.967	0.978	1.071
$T_{28\text{-}27}$	0	1.1	1.068	0.979	0.961	0.933
QC_{10}	0	5	0	4.947	1.737	3.286
QC_{12}	0	5	0	5.000	4.275	1.221
QC_{15}	0	5	0	3.254	4.737	4.601
QC_{17}	0	5	0	4.356	4.961	1.082
QC_{20}	0	5	0	4.598	1.584	0.444
QC_{21}	0	5	0	4.994	4.971	0.399
QC_{23}	0	5	0	4.954	3.703	2.446
QC_{24}	0	5	0	4.833	4.457	4.753
QC_{29}	0	5	0	4.997	4.998	3.887
L_{max}	–	–	0.1723	**0.1127**	0.1136	0.1180

The significance of bold text represent best value of fitness function in the table.

Table 15
Comparison of active power transmission losses obtained with different algorithms.

Method	Active power loss (MW)	Method description
HPSO-MVO	**2.854**	Hybrid Particle Swarm Optimization-Multi Verse Optimizer
MVO	2.881	Multi Verse Optimizer
PSO	3.026	Particle Swarm Optimization
BHBO	3.503	Black Hole- Based Optimization [7]

The significance of bold text represent best value of fitness function in the table.

Please cite this article in press as: P. Jangir et al., A novel hybrid Particle Swarm Optimizer with multi verse optimizer for global numerical optimization and Optimal Reactive Power Dispatch problem, Eng. Sci. Tech., Int. J. (2016), http://dx.doi.org/10.1016/j.jestch.2016.10.007

Table 16
Optimal values of control variables for case 4 with different algorithms.

Control variable	Min	Max	Initial	PSO-MVO	MVO	PSO
P_{G1}	50	200	99.2230	51.271	51.327	51.427
P_{G2}	20	80	80	80.000	80.000	80.000
P_{G5}	15	50	50	50.000	50.000	50.000
P_{G8}	10	35	20	34.999	35.000	35.000
P_{G11}	10	30	20	30.000	30.000	30.000
P_{G13}	12	40	20	40.000	40.000	40.000
V_{G1}	0.95	1.1	1.05	1.100	1.100	1.100
V_{G2}	0.95	1.1	1.04	1.098	1.097	1.100
V_{G5}	0.95	1.1	1.01	1.079	1.081	1.083
V_{G8}	0.95	1.1	1.01	1.087	1.088	1.090
V_{G11}	0.95	1.1	1.05	1.100	1.100	1.100
V_{G13}	0.95	1.1	1.05	1.100	1.100	1.100
$T_{4\text{-}12}$	0	1.1	1.078	1.007	1.037	0.977
$T_{6\text{-}9}$	0	1.1	1.069	0.943	0.901	1.100
$T_{6\text{-}10}$	0	1.1	1.032	0.988	0.994	1.100
$T_{28\text{-}27}$	0	1.1	1.068	0.982	0.987	0.998
QC_{10}	0	5	0	5.000	0.306	4.065
QC_{12}	0	5	0	4.556	3.082	0.000
QC_{15}	0	5	0	4.436	4.552	5.000
QC_{17}	0	5	0	4.826	0.815	5.000
QC_{20}	0	5	0	3.321	2.787	0.000
QC_{21}	0	5	0	4.856	1.106	5.000
QC_{23}	0	5	0	4.790	4.987	5.000
QC_{24}	0	5	0	4.470	2.308	0.000
QC_{29}	0	5	0	4.868	3.825	0.000
PLoss (MW)	–	–	5.8219	**2.854**	2.881	3.026

The significance of bold text represent best value of fitness function in the table.

Table 17
Comparison of reactive power losses obtained with different algorithms.

Method	Reactive power loss (MVAR)	Method description
HPSO-MVO	**−25.184**	Hybrid Particle Swarm Optimization-Multi Verse Optimizer
MVO	−25.038	Multi Verse Optimizer
PSO	−23.407	Particle Swarm Optimization
BHBO	−20.152	Black Hole- Based Optimization [7]

The significance of bold text represent best value of fitness function in the table.

Table 18
Optimal values of control variables for case 5 with different algorithms.

Control variable	Min	Max	Initial	PSO-MVO	MVO	PSO
P_{G1}	50	200	99.2230	51.324	51.348	51.644
P_{G2}	20	80	80	80.000	80.000	80.000
P_{G5}	15	50	50	50.000	50.000	50.000
P_{G8}	10	35	20	35.000	35.000	35.000
P_{G11}	10	30	20	29.994	29.998	30.000
P_{G13}	12	40	20	40.000	40.000	40.000
V_{G1}	0.95	1.1	1.05	1.100	1.100	1.100
V_{G2}	0.95	1.1	1.04	1.100	1.100	1.100
V_{G5}	0.95	1.1	1.01	1.092	1.093	1.100
V_{G8}	0.95	1.1	1.01	1.100	1.100	1.100
V_{G11}	0.95	1.1	1.05	1.099	1.100	1.100
V_{G13}	0.95	1.1	1.05	1.100	1.100	1.100
$T_{4\text{-}12}$	0	1.1	1.078	0.998	1.000	0.962
$T_{6\text{-}9}$	0	1.1	1.069	0.969	0.937	1.100
$T_{6\text{-}10}$	0	1.1	1.032	0.987	0.993	0.961
$T_{28\text{-}27}$	0	1.1	1.068	0.981	0.983	0.964
QC_{10}	0	5	0	4.806	0.775	5.000
QC_{12}	0	5	0	0.313	3.857	0.000
QC_{15}	0	5	0	4.997	3.668	0.000
QC_{17}	0	5	0	5.000	2.923	0.000
QC_{20}	0	5	0	5.000	4.170	0.000
QC_{21}	0	5	0	5.000	2.113	0.000
QC_{23}	0	5	0	4.923	3.390	0.000
QC_{24}	0	5	0	5.000	5.000	5.000
QC_{29}	0	5	0	2.293	2.952	0.000
QLoss (MVAR)	–	–	−4.6066	**−25.184**	−25.038	−23.407

The significance of bold text represent best value of fitness function in the table.

5.2.5. Case 5: Minimization of reactive power transmission losses

The accessibility of reactive power is the main point for static system voltage stability margin to support the transmission of active power from source to sinks [7].

Thus, the minimization of *VAR* losses are given by the following expression:

$$J = \sum_{i=1}^{NGen} Q_i = \sum_{i=1}^{NGen} Q_{Gi} - \sum_{i=1}^{NGen} Q_{Di} \tag{42}$$

It is notable that the reactive power losses are not essentially positive. The variation of reactive power losses with different methods shown in Fig. 28. It demonstrates that the suggested method has good convergence characteristics. The statistical values of reactive power losses obtained with different methods are shown in Table 17 which displays that the results obtained by hybrid PSO-MVO method is better than the other methods. The optimal values of control variables obtained by different algorithms for case 5 are given in Table 11. It is shown that the reactive power losses are greatly reduced compared to the initial case [7] from −4.6066 to −25.184 using hybrid PSO-MVO method.

6. Conclusion

Hybrid Particle Swarm Optimization-Multi Verse Optimizer (HPSO-MVO), Multi Verse Optimizer and Particle Swarm Optimization Algorithm are successfully applied to unconstrained benchmark function and standard IEEE 30-bus test systems to solve the Optimal Reactive Power Dispatch problem for the various types of cases. The results gives the optimal settings of control variables with different methods which demonstrate the effectiveness of the different techniques. The solutions obtained from the hybrid PSO-MVO method approach has good convergence characteristics and gives the better results compared to MVO and PSO methods which confirms the effectiveness of proposed algorithm.

Conflict of Interests

The authors declare that there is no conflict of interests regarding the publication of this paper.

Acknowledgment

The authors would like to thank Prof. Seyedali Mirjalili for his valuable comments and support. http://www.alimirjalili.com/MVO.html.

References

[1] H.R.E.H. Bouchekara, M.A. Abido, A.E. Chaib, R. Mehasni, Optimal reactive power dispatch using the league championship algorithm: a case study of the Algerian power system, Energy Convers. Manag. 87 (2014) 58–70.
[2] S. Duman, U. Güvenç, Y. Sönmez, N. Yörükeren, Optimal reactive power dispatch using gravitational search algorithm, Energy Convers. Manag. 59 (2012) 86–95.
[3] T. Niknam, R. Narimani, M. Jabbari, A.R. Malekpour, A modified shuffle frog leaping algorithm for multi-objective optimal reactive power dispatch, Energy 36 (11) (2011) 6420–6432.
[4] J. Carpentier, Contribution à l'étude du Dispatching Economique, Bull. Soc. Fr. Electriciens (1962) 431–447.
[5] H.R.E.H. Bouchekara, M.A. Abido, M. Boucherma, Optimal reactive power dispatch using teaching-learning-based optimization technique, Electr. Power Syst. Res. 114 (2014) 49–59.
[6] A.A. Abou El Ela, M.A. Abido, Optimal reactive power dispatch using differential evolution algorithm, Electr. Power Syst. Res. 80 (7) (2010) 878–885.
[7] H.R.E.H. Bouchekara, Optimal power flow using black-hole-based optimization approach, Appl. Soft Comput. 24 (2014) 879–888.
[8] S. Frank, I. Steponavice, S. Rebennack, Optimal reactive power dispatch: a bibliographic survey I, formulations and deterministic methods, Energy Syst. 3 (3) (2012) 221–258.

Please cite this article in press as: P. Jangir et al., A novel hybrid Particle Swarm Optimizer with multi verse optimizer for global numerical optimization and Optimal Reactive Power Dispatch problem, Eng. Sci. Tech., Int. J. (2016), http://dx.doi.org/10.1016/j.jestch.2016.10.007

[9] M.R. AlRashidi, M.E. El-Hawary, Applications of computational intelligence techniques for solving the revived optimal reactive power dispatch problem, Electr. PowerSyst. Res. 79 (4) (2009) 694–702.
[10] S. Frank, I. Steponavice, S. Rebennack, Optimal reactive power dispatch: a bibliographic survey II, non-deterministic and hybrid methods, Energy Syst. 3 (3) (2012) 259–289.
[11] A.R. Yildiz, A comparative study of population-based optimization algorithms for turning operations, Inf. Sci. (NY) 210 (2012) 81–88.
[12] J. Kennedy, R. Eberhart, Particle swarm optimization, Proceedings of the IEEE International Conference on Neural Networks, Perth, Australia, 1995, pp. 1942–1948.
[13] Seyedali Mirjalili, Seyed Mohammad Mirjalili, Abdolreza Hatamlou, Multi-Verse Optimizer: a nature-inspired algorith for global optimization, The Natural Computing Applications Forum 2015, 17 March 2015 doi: 10.1007/s00521-015-1870-7.
[14] K. Lee, Y. Park, J. Ortiz, A united approach to optimal real and reactive power dispatch, IEEE Trans. Power App. Syst. 104 (5) (1985) 1147–1153.
[15] P. Kessel, H. Glavitsch, Estimating the voltage stability of a power system, IEEE Trans. Power Deliv. 1 (3) (1986) 346–354.
[16] A.G. Bakirtzis, P.N. Biskas, C.E. Zoumas, V. Petridis, Optimal reactive power dispatch by enhanced genetic algorithm, IEEE Trans. Power Syst. 17 (2) (2002) 229–236.
[17] W. Ongsakul, T. Tantimaporn, Optimal reactive power dispatch by improved evolutionary programming, Electr. Power Compon. Syst. 34 (1) (2006) 79–95.
[18] C.A. Belhadj, M.A. Abido, An optimized fast voltage stability indicator, Electric Power International Conference on Engineering, PowerTech Budapest, 1999, pp. 79–83.
[19] S.A.H. Soliman, A.H. Mantawy, Modern Optimization Techniques With Applications in Electric Power Systems, Energy Systems, Springer, New York/Heidelberg/Dordrecht/London, 2012.
[20] T. Bouktir, R. Labdani, L. Slimani, Optimal reactive power dispatch of the Algerian electrical network using ant colony optimization method, Leoanardo J. Sci. (2005) 43–57.

Please cite this article in press as: P. Jangir et al., A novel hybrid Particle Swarm Optimizer with multi verse optimizer for global numerical optimization and Optimal Reactive Power Dispatch problem, Eng. Sci. Tech., Int. J. (2016), http://dx.doi.org/10.1016/j.jestch.2016.10.007